Title

Si-H vibrational mode on a H-Si(111)1×1 surface with hydrogen deficiency

Author

Yoshihiro Miyauchi, Khuat Thi Thu Hien, and Goro Mizutani*

Affiliations

School of Materials Science, Japan Advanced Institute of Science and Technology,
1-1 Asahidai, Nomi, Ishikawa 923-1292, JAPAN
E-mail: y-miyau@jaist.ac.jp, Tel: +81-761-51-1152, FAX: +81-761-51-1149

Abstract

We used a dipole coupling theory to calculate modulations of the Si-H vibrational mode on a H-Si(111)1×1 surface, and analyzed the observed optical sum frequency generation (SFG) spectra. As the hydrogen coverage decreased the peak position of the Si-H vibrational mode shifted to the red side in the experimental SFG spectra [Hien et al, Surf. Int. Anal., **44** 662 (2012)]. The calculated peak shift was quantitatively consistent with the observed redshift, indicating that the peak shift can be attributed to dipole coupling among the Si-H oscillators. On the other hand, the experimental peak widths at lower coverages were wider than those of the calculated peaks. This suggests that local structural defects and/or dangling bonds modulated the vibration of the surrounding Si-H oscillators.

Keywords

Dipole-dipole interaction; Sum frequency generation; Hydrogen; Silicon; Vibration

1. Introduction

One of the central processes of the chemical vapor deposition (CVD) of a high quality amorphous Si layer (a-Si) on a Si crystal surface is hydrogen desorption from the hydrogen terminated surface [1]. Recombinative hydrogen desorption processes from H-Si(100)3×1, H-Si(100)2×1, H-Si(111)7×7 surfaces have been vigorously studied by several techniques, including temperature programmed desorption (TPD) [2,3], laser-induced thermal desorption (LITD) [4-7], scanning tunneling microscopy (STM) [8,9], optical second harmonic generation (SHG) [10-11] and Fourier transform infrared spectroscopy (FT-IR) [12,13].

Chemical hydrogen termination on a Si surface is commonly used to protect the surface from oxidization before the CVD process. The hydrogen layer is removed from this Si surface in the initial process of the CVD growth. However, a number of studies report that the desorption process from a H-Si(111)1×1 surface [17-24] is much smaller than those from Si(111)7×7 and other surfaces. The process on the H-Si(111)1×1 surface is complicated, and still not well understood, since the termination itself influences the structure and the chemical reactions.

Scanning tunneling microscopy (STM) of a H-Si(111)1×1 surface after electron bombardment with an energy of 2~10 eV produced results consistent with the typical complexity of the desorption process [17]. Namely, the bombardment induced hydrogen atomic desorption, and then the resulting 1×1 structure changed into quasi-stable 2×1 due to the free energy of the dangling bonds created at the vacancy site. Hence the electron-stimulated desorption (ESD) directly broke the Si-H bonds. The direct breaking process induced the change of the electronic states and the surface reconstruction.

Hydrogen recombinative desorption by thermal excitation from the surface should be more complicated. Knowing how the thermal desorption proceeds on a H-Si(111) 1×1 surface is critical for understanding the elementary steps in the CVD growth of a-Si. Renzi and his colleagues studied the dynamics on a 1×1 surface by using low energy electron diffraction (LEED), ultra-violet photoemission spectroscopy (UPS), and high resolution electron energy loss spectroscopy (HREELS) [20]. Below 738 K, they found upward band bending due to the creation of a small number of dangling bonds but they observed no structural change from 1×1. When the temperature increased from 773 to 973 K all hydrogen was desorbed, and the surface began to reconstruct. Above 873 K, the band bending decreased, the 7×7 reconstruction became predominant, and an adatom state was progressively formed. Vinh et al., who used reflection high energy electron diffraction (RHEED) patterns, also observed no intrinsic structural change of the

surface below 823 K [18]. These studies indicate the electronic and structural change via hydrogen desorption. However, it is still unclear how the changes of the structure and the electronic states give feedback to the bonding states of the monohydride.

Hydrogen desorption requires the breaking of the bonds. Thus, the change of the bonding states during the desorption process must be investigated. Si-H bonds on the Si(111)1×1 surface have big dipole moments and interact with each other via dipole coupling [22, 23]. Thus, the bonds are influenced not only by the electronic states in the Si-H structures, but also by the coverage and the domain structures [23]. Renzi and colleagues observed Si-H vibrational modes by using HREELS with an energy resolution of ~100 cm^{-1}, but did not observe any modulation of the vibrational peaks except intensity reduction.

Previously, we obtained isothermal desorption spectra of the H-Si(111)1×1 surface at 711~771 K by probing vibrationally resonant optical sum frequency generation (SFG) [24]. As a result, redshift of the Si-H vibrational peak position and inhomogeneous broadening were observed with the reduction of hydrogen coverage [24,25]. However, the origins of these spectral modulations were not clarified. In this study, we analyze the modulations using a theory of dipole coupling [26]. The results show that these modulations are caused by an increased number of random hydrogen vacancy sites after the hydrogen desorption.

2. Experimental and Calculation

A detailed description of the experimental methodology has already been published [24,25]. Briefly, the n-type Si(111) wafer was terminated by a well-known chemical treatment [14]. After that, the sample was immediately introduced into an ultra-high vacuum (UHV) chamber with pressure of ~10^{-5} Pa. The sample was heated for ~10 s several times. After each heating, the SFG spectrum of the Si surface at room temperature was taken. The polarizations of the SFG, visible and IR light beams were *s*, *s*, and *p*, respectively. The peaks attributed to the Si-H stretching vibration in the SFG spectra were fitted using the equation

$$\chi^{SFG} = \chi^{NR} e^{i\varphi} + \frac{\chi_v}{\omega - \omega_v + i\gamma}. \quad (1)$$

Here $\chi^{NR}, \chi_v, \varphi, \omega_v$, and γ are nonlinear susceptibility, total hyperpolarizability of the Si-H molecules, phase difference between the resonant and non-resonant terms, the resonant frequency, and the damping constant of the resonant mode, respectively [21].

The line width of our IR probe light was ~3 cm^{-1}, but the energy fluctuation limit in

practice has been reported as ±0.15cm^{-1} [26]. In order to find the fluctuation of the probe light tuning in our system, we took SFG spectra of eight different samples, and determined the center peak positions and the widths of the Si-H vibrational peaks. The standard deviations of the peak positions and widths were 0.15 and 0.23 cm^{-1}, respectively. In addition, peak shift and width broadening with 0.1 cm^{-1} order were clearly measured in our previous report [24]. Thus, we suggest that in practice, the fluctuation limit of our system was at least better than 0.3 cm^{-1}.

A simulation of the dipole-dipole interaction using coherent potential approximation (CPA) was developed by Persson and Ryberg [27]. The calculation of nonlinear susceptibility based on the CPA method has been reported by Backus [28], Backus and Bonn[29], and Cho, Hess, and Bonn [30]. The calculated susceptibility well described an experimental SFG spectrum. We calculated the nonlinear susceptibility using their method; the Appendix shows how we chose the detailed parameters for simulating the H-Si(111)1×1 surface.

3. Results and discussion

We calculated the θ-χ_v relation of the hydrogenated Si surface and the result is shown as the solid curve in Fig. 1. The coverage θ of the hydrogen atoms on the H-Si(111) surface could be approximately expressed as [21, 24]

$$\theta \propto \sqrt{I_{SFG}} \propto \chi_v \quad . \tag{2}$$

However, the relation in Eq. (2) does not hold, especially in the presence of strong dipole coupling between oscillators [28-31]. The value of χ_v is not proportional to the coverage θ in a precise sense. We use this relation in Fig. 1 for determining the coverage in this study.

Figure 2 shows an experimental isothermal desorption spectrum of the H-Si(111)1×1 surface at 722 K. The detailed description of the spectrum was reported in Ref. [24]. The plots show the coverage and the error bars are standard deviations when we fit the SFG signals to Eq. (1). The solid curve represents the result of fitting by second-order hydrogen desorption as

$$\frac{d\theta}{dt} = -k\theta^2. \tag{3}$$

Eq. (3) yields $\theta = \frac{1}{kt+1}$. Here t is the heating time and k represents the desorption rate. The reduction of the coverage is well-described as second-order desorption, and thus at least the desorption process is consistent with that on the Si(111)7×7 surface [4,7,10]. In the second-order process, one hydrogen atom leaves a Si atom and diffuses toward another Si-H site where they

combine to form a dihydride (Si-H_2). For a while, the dihydride state sustains. Finally the hydrogen atoms go beyond the highest potential barrier in the reaction coordinate, associate themselves with each other and desorb from the Si atom [32]. In this way, the hydrogen recombinative desorption occurs at a single Si atom. The vacancy sites are thus created randomly on the Si surface in a microscopic scale. The remaining Si-H bonds on the surface do not have translational invariance due to the random vacancy sites, and theoretically their vibration should be reproducible by the CPA method.

In order to study the modulation of the polarizability, we investigated the change of the Si-H vibrational peak shapes in the SFG spectra. Figures 3 (a) and (b) show experimental and theoretical SFG spectra as a function of the coverage. While the SFG spectra in Fig. 3(a) are in the region from 2070 to 2100 cm^{-1}, the SFG spectra in Fig. 3(b) were drawn in the region from 2080 to 2085 cm^{-1}. In both panels, peaks are seen at 2083.7 cm^{-1} at 1ML, and then the peak intensities weaken at lower hydrogen coverages. The peak positions of the spectra are shifted toward the lower frequency side. The experimental peaks broadened significantly at coverages below 0.85 ML, while the theoretical peaks maintained their sharpness. A peak shift and inhomogeneous broadening were observed in the SFG spectra at temperatures from 711 to 771 K [24]. We note that the SFG measurements were performed at room temperature with sufficient cooling down after the heating, and thus these modulations are not due to coupling with phonons [33].

Figures 4 (a) and (b) show the peak positions and the widths of the SFG spectra in Fig. 3 as a function of coverage. The points represent experimental results, while solid curves show theoretical ones. The full width of half maximum (FWHM) of the experimental peak width is 3.2 cm^{-1} at 1 ML, as shown in Fig. 4(b). The incident line width was incorporated in the theoretical width in Fig. 4(b) using the Voigt function as:

$$I^{SFG} \propto \left| \int_{-\infty}^{\infty} G(\omega_{IR} - \tau)\chi^{(2)}(\tau)d\tau \right|^2. \quad (4)$$

Here $G(\omega)$ is a Gaussian function with the full width at half maximum of 3 cm^{-1}. The inset in Fig. 4(b) shows the calculated peak width with a magnified vertical scale.

In Fig. 4(a), the red-shifting theoretical curve is quantitatively consistent with the experimental peak positions. This indicates that the peak shift is attributed to the modulation of the polarizability of the singular Si-H oscillators via dipole coupling with the increase of vacancy sites.

On the other hand, in Fig. 4(b), the experimental peak widths are far wider than the theoretical ones. In the inset of Fig. 4(b), the calculated width is seen to increase only by 0.001 cm^{-1} order as a function of the hydrogen deficiency via dipole coupling. The calculated width is

~3.25 cm^{-1} at 0.45 ML. However, the experimental width broadenings at coverages below 0.79 ML are far wider than the calculated ones. As an example, the experimental width was ~8 cm^{-1} at 0.48 ML.

We would like to note that the width broadening of ~1 cm^{-1} in the IR spectra of the H and D terminated Si(111) surface was mainly due to the dipole couplings of Si-H and Si-D molecules [22]. The experimental broadening of ~8cm^{-1} observed in this study is much larger than ~1 cm^{-1}, and thus, the observed broadening at low coverages in Fig. 3(a) cannot be explained by the dipole coupling effect.

As the first step toward understanding the origin of the width broadening, we needed to ascertain whether the broadening should be classified as homogeneous or inhomogeneous. We fitted the experimental vibrational peaks by Gaussian and Lorentzian functions, and then evaluated the Pearson's correlation coefficient *r* among the experimental and fitted curves [34]. At 1 ML, the coefficient *r* for the case of a Gaussian curve was 0.980, while the *r* for the case of a Lorentzian curve was 0.993. Thus, the experimental peak at 1 ML was judged to have pure homogeneous broadening. With reduction of coverage, the coefficient *r* for the case of Gaussian curves gradually increased, becoming ~0.99 at 0.58 ML. This value is the same as the *r* for the case of Lorentzian curves. This indicates that the spectra contained inhomogeneous broadenings at coverages lower than 0.58 ML.

According to Chabal et al., there are three candidate origins of the inhomogeneous broadening of hydrogen vibration on a Si surface [23].

(a) Point defects such as foreign atoms and local structural defects in the microscopic scale.
(b) Mesoscopic defects due to finite size domains and the boundary
(c) Extrinsic macroscopic inhomogeneities such as spatial and/or temporal variations of temperature, coverage, distribution, domain size, and density of point defects.

Considering these candidates in reverse order, the inhomogeneous broadening observed in this study is not due to macroscopic inhomogeneities. With ~5 μm resolution, we observed SFG microscopic images of an area 200×200 μm^2 on the Si(111) surface at several surface temperatures [24]. The SFG intensity decreased at higher temperatures but showed isotropic spatial distribution at and below 728 K. This result indicates that candidate (c) is not feasible as the origin of the broadening.

Next, we discuss candidate (b). According to the simulation by Chabal et al., the vibrational peak of Si-H moves with dipole coupling between domains toward the red side with decrease of the domain size [23]. Due to the coupling between the domains, a Si-H peak on the H-Si(111) surface can have asymmetric inhomogeneous broadening. However, this

inhomogeneous width was 0.07 cm^{-1} at 70 K on the surface observed by ATR-FTIR measurement with 0.04 cm^{-1} resolution [22], and it was far smaller than the width ~8 cm^{-1} at 0.48 ML in this study. In fact, no modulation of the Si-H vibrational mode caused by the change of domain size was observed by Luo et al. [22]. Thus, candidate (b) also can be excluded as the origin of the broadening.

The only remaining candidate for the origin of the inhomogeneous broadening is point defects, as categorized in (a). Since the 1×1 structure remains at least below 738 K, only local structural defects can influence the Si-H vibration. Point defects such as oxidization due to adsorption of impurities are not applicable here because the sample was kept in a high vacuum of 10^{-5} Pa. Ye and his colleagues used SFG to study laser-induced oxidization of the Si surface in ambient conditions [21]. With an increase of laser irradiation time, the nonlinear susceptibility χ_v of the SFG signal reduced, but neither peak shift nor width broadening was observed in the spectra. Thus, oxidization due to impurities adsorption does not modify the peak shape, and local structural defects at the vacancy sites remain as the origin of the broadening.

In their discussion of candidate origins, Chabal et al. [23] note that point defects could be the main origin of the experimental inhomogeneity. In addition, we point out that the dangling bonds created after hydrogen desorption may influence the electronic states and orientation of neighboring Si-H bonds. The frequency of a Si-H oscillator could be changed with an increase of neighboring dangling bonds. Hence, we suggest that while oxidization on the surface is not adaptable, the point defects and/or the dangling bonds are feasible candidates as origins of the inhomogeneity. In order to understand the inhomogeneity more clearly, we should use a quantum mechanical simulation to analyze the frequency change of a Si-H oscillator as a function of the number of neighboring dangling bonds. This will be the subject of a future study.

The experimental inhomogeneity indicates that many kinds of Si-H oscillators emerged on the surface at lower coverages. On the other hand, the peak position shift observed by the experiment is in good agreement with our calculations. Thus, we suggest that the many kinds of oscillators corresponding to the experimental inhomogeneity could be approximately treated as a single oscillator modeled by our calculation, so far as their mean susceptibility is concerned.

4. Conclusions

In this study, we have calculated modulation of the Si-H vibrational mode on a Si(111) 1×1 surface by a partial absence of Si-H bonds, and made a comparison between modulations in the

experimental and theoretical SFG spectra of the surface. A theoretical peak shift reproduced the experiment quantitatively, and thus the peak shift was due to the modulation of average polarizability of the Si-H oscillators via dipole coupling. On the other hand, inhomogeneous broadenings of the theoretical peaks in the SFG spectra at lower coverages were much larger than those of the calculated peaks.

5. Appendix

The derivation of nonlinear susceptibility χ by a simulation of dipole-dipole interaction has already been reported elsewhere [28-30]. Thus, here we only explain how we chose parameters for the calculation of a H-Si(111)1×1 surface.

When an outer field E_i irradiates the sample, the dipole moment of an oscillator at x_i on a surface is written as

$$p_i = \alpha(E_i - \sum_{j \neq i} U_{ij} p_j), \quad \text{(A1)}$$

where $U_{ij}p_j$ is the electric field at $\vec{x}_i$ from a dipole p_j at $\vec{x}_j$. U_{ij} is written as

$$U_{ij} = \frac{1}{|\vec{x}_i - \vec{x}_j|^3} + \ldots. \quad \text{(A2)}$$

If the system has translational invariance, the Fourier transformed dipole moment p_q and the total polarizability α_0 are

$$p_q = \frac{\alpha}{1+\alpha\tilde{U}(\vec{q})} E_q \equiv \alpha_0(\vec{q},\omega) E_q. \quad \text{(A3)}$$

The $\tilde{U}(\vec{q})$ is written as

$$\tilde{U}(\vec{q}) = \sum_j U_{ij} \exp(-i\vec{q} \cdot (\vec{x}_i - \vec{x}_j)). \quad \text{(A4)}$$

Here $\vec{q}$ is a vector in the momentum space [26].

If the translational invariance of the system is broken due to the coexistence of isotopes or the existence of vacancy sites, it is difficult to obtain the polarizability analytically. Thus, Persson and Ryberg proposed a simplified method using coherent potential approximation (CPA) [27]. In CPA, the ensemble of all possible configurations is represented by a system based on an average molecule at each site.

According to CPA theory, the ensemble average polarizability α on a surface can be

calculated by the self-consistent equation [27-30]

$$\sum_{\mu} \frac{c_{\mu}\alpha_{\mu}}{1+(\alpha_{\mu}-\alpha)Q} = \alpha. \qquad \text{(A5)}$$

Here α_{μ} is the polarizability of an oscillator μ, and c_{μ} represents the coverage of the oscillator μ on a solid surface. When we calculated the average polarizability α, we assumed that oscillators with only one singular Si-H vibrational mode are on the H-Si(111) surface. The Q value [27-30] is

$$Q = \frac{1}{A^*}\int_{BZ} d^2q \frac{\tilde{U}(\vec{q})}{1+\alpha\tilde{U}(\vec{q})} \qquad \text{(A6)}$$

where, A^* is the area of the 1st Brillouin zone. In order to calculate the Q value, we approximated $\tilde{U}(\vec{q})$ as the quadratic function

$$\tilde{U}(\vec{q}) = U_0[1 + A\frac{q}{q_0} + B(\frac{q}{q_0})^2] \qquad \text{(A7)}$$

with the direction q[10]=q[11] in case of the Si surface. The q_0 is the radius of a circular area πq_0^2, and the latter is the same as the area $A^* = \left[\frac{2\pi}{a}\right]^2$. Here a is the distance among the Si-H oscillators, and it is 3.84 Å [23]. We used eq. (A4) to calculate the values of $\tilde{U}(\vec{q})$ from the distance. The results are shown as solid dots in Fig. 5. The vertical axis is the strength of $\tilde{U}(\vec{q})$, and the horizontal axis represents the wavenumber q along [11] direction. By fitting $\tilde{U}(\vec{q})$ with eq. (A7), we obtained U_0=0.17 Å^{-3}, A=-3.04, and B=1.56. We note that we calculated the $\tilde{U}(\vec{q})$ while changing the height of the image plane, but there were few differences in $\tilde{U}(\vec{q})$. Thus, we neglect dipoles on the image plane in this calculation.

Then, we calculated the integral Q after having $\tilde{U}(\vec{q})$ [27-30].

The polarizability α_{μ} in Eq. (6) is written as

$$\alpha_{\mu} = \alpha_e + \frac{\alpha_v}{1-(\omega/\omega_{\mu})(\omega/\omega_{\mu}+i\gamma)}. \qquad \text{(A8)}$$

Here α_e is the electronic polarizability, α_v is the vibrational polarizability, ω_μ is the resonance frequency and γ is the damping constant. Chabal et al. estimated the value of α_e as 5.7 Å ^{3} [23]. The dynamic dipole moment was also measured as 0.1D [13], and thus α_v should be 0.043 Å ^{3} [35].

We chose a theoretical peak width of 0.1 cm^{-1}. The experimental peak width is observed as 3.2 cm^{-1} at 1ML, but this is an extrinsic width due to our optical system, especially our OPG/DFG source. The intrinsic width of the Si-H bond is 0.9 cm^{-1} at room temperature [14]. The width is broadened due to the coupling of the Si-H stretching vibration with a bending mode and an optical phonon [33]. In this calculation, we treat only one Si-H oscillator, and thus we should consider only lifetime broadening. The observed lifetime broadening of the Si-H vibrational peak width is less than 0.005cm^{-1} [23]. However, this width is much smaller than the limitation of wavenumber step size in our calculation. We therefore set the width as 0.1cm^{-1} in this calculation.

We set another adjustable parameter ω_μ as 2079.8 cm^{-1}. After obtaining the average polarizability α by calculating Eqs. (A5) and (A6), we got the total polarizability α_0 by inserting α into Eq. (A3).

References

[1] A. H. Mahan, Y. Xu, D. L. Williamson, W. Beyer, J. D. Perkins, M. Vanecek, L. M. Gedvilas and B. P. Nelson, *J. Appl. Phys*. **90**, 5038 (2001).

[2] A. Namiki, *Progress in Surf. Sci.*, 81, 337 (2006).

[3] M. C. Flowers, N. B. H. Jonathan, Y. Liu, and A. Morris, *J. Chem. Phys.* **1995**, *102*, 1034.

[4] B. G. Koehler, C. H. Mak, D. A. Arthur, P. A. Coon, and S. M. George, *J. Chem. Phys*. **1988**, *89(3)*, 1709.

[5] K. Sinniah, M. G. Sherman, L. B. Lewis, W. H. Weinberg, J. T. Yates, Jr., and K. C. Janda, *Phys. Rev. Lett*. ***62***, 567, (1989).

[6] K. Sinniah, M. G. Sherman, L. B. Lewis, W. H. Weinberg, J. T. Yates, Jr., and K. C. Janda, *J. Chem. Phys*. ***92***, 5700 (1990).

[7] M. L. Wise, B. G. Koehler, P. Gupta, P. A. Coon, and S. M. George, *Surf. Sci.* **258**, 166 (1991).

[8] M. Dürr, M. B. Raschke, U. Höfer, T. F. Heinz, *Sci*. 296, 1838 (2002).

[9] Y. Morita, K. Miki, and H. Tokumoto, *Sur. Sci.* **1995**, *325*, 21.

[10] G. A. Reider, U. Hofer, and T. F. Heinz, *J. Chem. Phys*. **94**, 4080 (1991).

[11] G. A. Reider, U. Höfer, and T. F. Heinz, *Phys. Rev. Let.* **66**, 1994 (1991).

[12] M. Niwano, M. Terashi, J. Kuge, *Surf. Sci*. 420, 6 (1999).

[13] P. Gupta, V. L. Colvin, and S. M. George, *Phys. Rev. B**37***, 8234 (1988),.

[14] G. S. Higashi, Y. J. Chabal, G. W. Trucks, and K. Raghavachari, *Appl. Phys. Let*. **56**, 656 (1990).

[15] P. Guyot-sionnest, *Phys. Rev. Let*., 66 1489 (1991).

[16] A. Kawasuso, M. Yoshikawa, K. Kojima, S. Okada, and A. Ichimiya, *Phys. Rev*. B**61**, 2102 (2000).

[17] R. S. Becker, G. S. Higashi, Y. J. Chabal, and A. J. Becker, *Phys. Rev. Let*. 65, 1917 (1990).

[18] L. Vinh, M. Eddrief, ,C. A. Sebenne, P. Dumas, A. Taleb-Ibrahimi, R. Gunther, Y. J. Chabal, J. Derrien, *Appl. Phys. Let*. **64**, 3308 (1994).

[19] A. Pusel, U. Wetterauer, and P. Hess, *Phys. Rev. Let*. 81, 645 (1998).

[20] V. D. Renzi, R. Biagi, and U. D. Pennino, *Surf. Sci*. **497,** 247 (2002).

[21] S. Ye, T. Saito, S. Nihonyanagi, K. Uosaki, P. B. Miranda, D. Kim, Y. R. Shen, *Surf. Sci*. 476, 121 (2001).

[22] H. Luo and C. E. D. Chidsey, *Appl. Phys. Let*. 72, 477 (1998).

[23] P. Jakob, Y. J. Chabal. And K. Raghavachari, *Chem. Phys. Let*. **187**, 325 (1991).

[24] K. Hien, Y. Miyauchi, M. Kikuchi, and G. Mizutani, *Surf. Int. Anal*. **44**, 662 (2012).

[25] Y. Miyauchi, *Phys. Res. Int*. **2012**, 57654-1 (2011).

[26] P. Guyot-Sionnest, *J. Electron . Spectrosc. Relat. Phenom*. **64-65**, 1 (1993).

[27] B. N. J. Persson, and R. Ryberg, *Phys. Rev. B* 24 6954 (1981).

[28] Backus, E. H. G., *Driving and probing surfaces with light* (Leiden University, 2005), pp. 119.

[29] E. H. G. Backus, and M. Bonn, *Chem. Phys. Lett.* 412, 152 (2005).

[30] M. Cho, C. Hess, and M. Bonn, *Phys. Rev. B* 65, 205423 (2002).

[31] S. Katano, A. Bandara, J. Kubota, K. Onda, A. Wada, K. Domen, and C. Hirose, *Surf. Sci*. **427**, 337 (1999).

[32] A. Vittadini, A. Sellloni, *Surf. Sci*. 383, L**779** (1997),

[33] P. Dumas, Y. J. Chabal and G. S. Higashi, *Phys. Rev. Let*. **65**, 1124 (1990).

[34] P. Yu, *Applied Spectroscopy* **59**, 1372 (2005).

[35] M. Morin, P. Jakob, N. J. Levinos, Y. J. Chabal, and A. L. Harris J., *Chem. Phys*. 96, 6203 (1992).

Acknowledgements

The authors would like to thank Prof. Emeritus A. Ichimiya of Nagoya University for his valuable advice. This work was supported in part by a Grant-in-Aid for Scientific Research (C) (#23540363) and Grant-in-Aid for Young Scientists (B) (#23740238) of Japan Society for the Promotion of Science.

Figure Captions

Fig. 1. Nonlinear susceptibility as a function of coverage on a Si(111)1×1 surface calculated by coherent potential approximation (CPA) method. The horizontal axis represents coverage, and the vertical one shows the absolute value of the nonlinear susceptibility χ. In this calculation, we set the wavenumber of an isolated Si-H oscillator as 2079.8 cm^{-1}, and the peak width as 0.1 cm^{-1}. We also set the distance between Si-H oscillators as 3.84 Å, and the permanent and dynamic dipoles as 5.7 and 0.043 $Å^3$, respectively. We simulated the nonlinear susceptibility using the calculation method reported by Backus and Bonn [29].

Fig. 2. An isothermal desorption spectrum from a Si(111)1×1 surface at 722 K. The horizontal axis shows time and the vertical represents hydrogen coverage on the Si surface. We fitted the SFG spectra at each time by eq. (1), obtained the nonlinear susceptibility χ, and then calculated the coverage using the χ-coverage relation shown in Fig.1. The solid dots are experimental results, and the error bars represent the standard deviation. The solid curve was fitted to the experiment by eq. (3).

Fig. 3. (a) Experimental and (b) calculated SFG spectra as a function of the coverage. The horizontal axis represents the wavenumber of the IR probe light and the vertical axis shows the SFG intensity. Hydrogen coverage is denoted on the left side of each SFG spectrum. The solid dots represent the observed SFG intensity and the curve represents the fitting by eq. (1). The SFG spectra were observed at room temperature after heating the sample to 722K. The polarizations of SFG, visible, and IR light were s, s, and p, respectively. The wavelength of the visible light was 532.1nm. The solid curves shown in (b) represent the SFG intensity calculated by the CPA method.

Fig. 4. (a) Peak position and (b) peak width of Si-H stretching vibration as a function of coverage. The horizontal axis shows the coverage obtained by fitting with eq. (1). Solid dots shown in (a) and (b) are the observed peak positions and widths. The error bars are standard deviations. Solid curves shown in (a) and (b) represent theoretical peak width and position, respectively. In (b), we show the width of a Voigt function convoluting intrinsic theoretical width and extrinsic width ~3cm^{-1} corresponding to the optical system. The inset shows theoretical peak width with the magnified

vertical scale of Fig. 4(b).

Fig. 5. U(q) of the dipole field for [11] direction in the two-dimensional Brillouin-zone on a Si(111) surface. The horizontal axis represents the wavenumber q along [11] direction and the vertical axis shows the strength of Fourier transformed $\tilde{U}(\vec{q})$ We obtained $\tilde{U}(\vec{q})$ by calculating eq. (A4) from the distance between 3.84 Å of the Si-H oscillators. The results are shown as solid dots. By fitting them with eq. (A7), we obtained the parameters U_0=0.17 Å^{-3}, A=-3.04, and B=1.56.

Figures

Figure 1

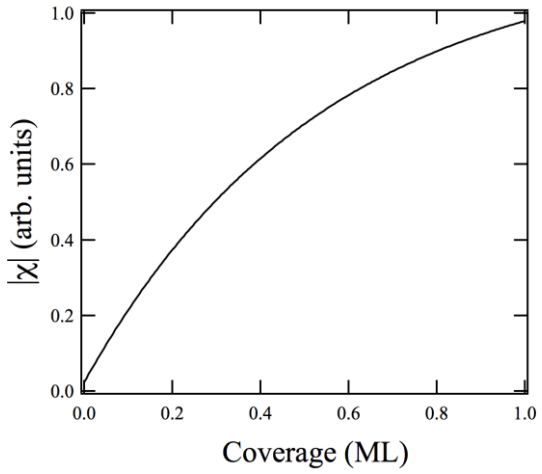

Figure 2

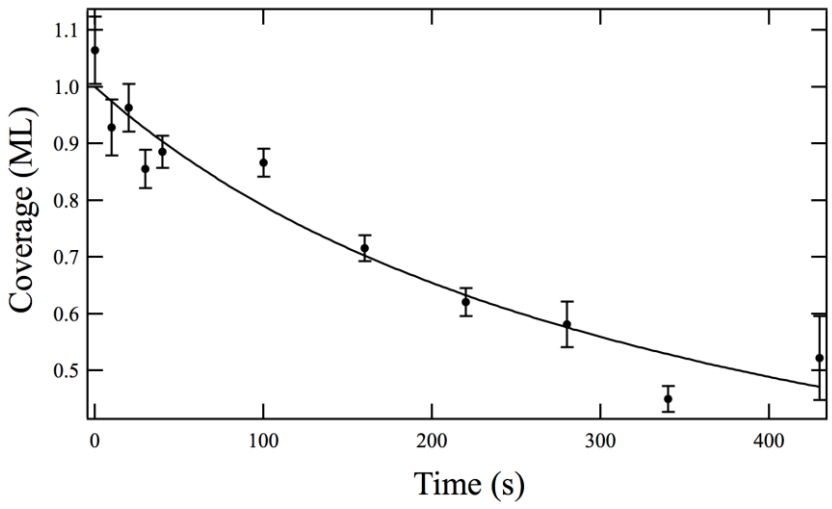

Figure 3

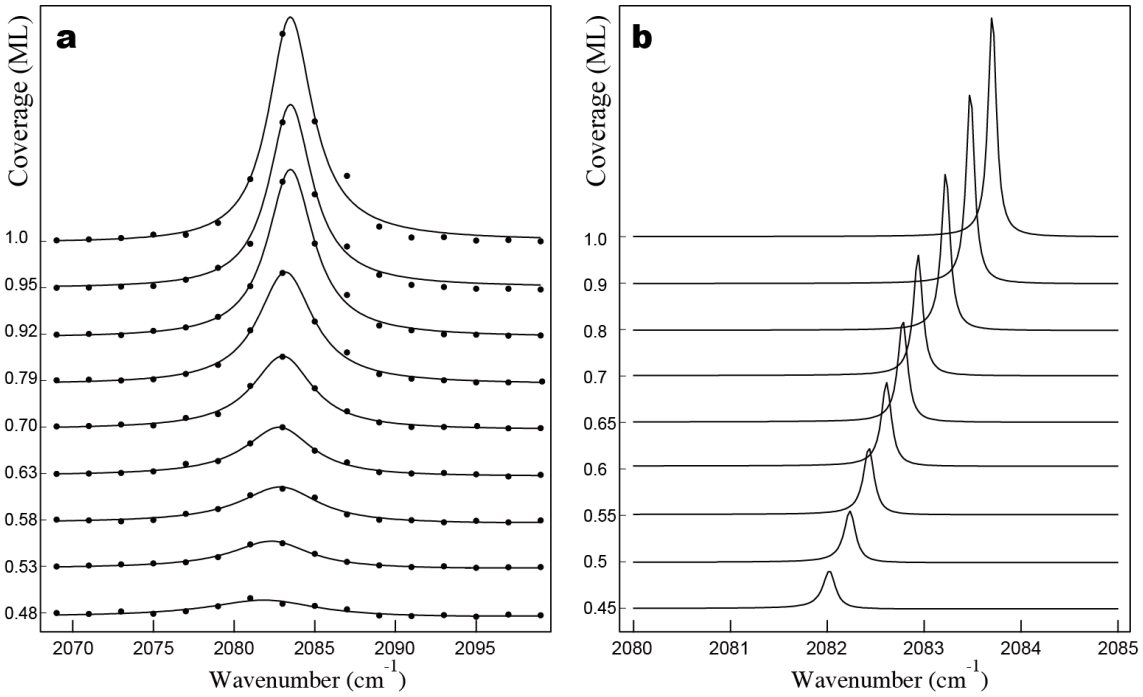

Figure 4

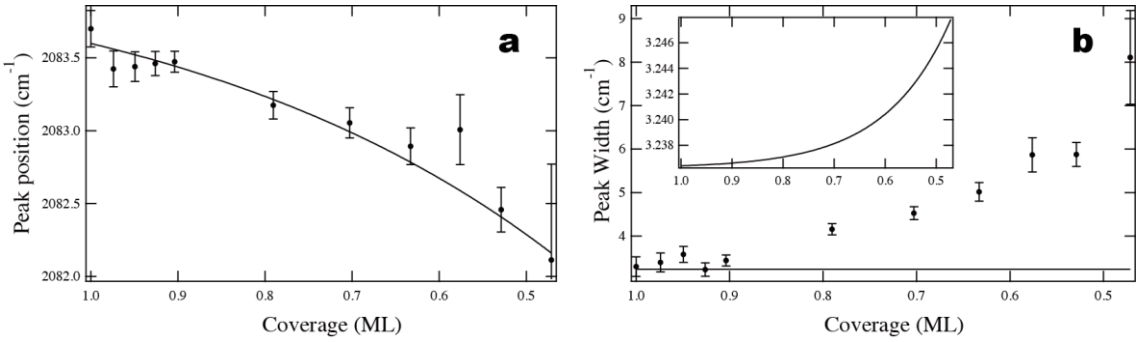

Figure 5